

Received June 16, 2017, accepted July 3, 2017, date of publication July 11, 2017, date of current version July 31, 2017.

Digital Object Identifier 10.1109/ACCESS.2017.2725301

State of Charge Estimation of Battery Energy Storage Systems Based on Adaptive Unscented Kalman Filter With a Noise Statistics Estimator

SIMIN PENG^{1,2}, (Member, IEEE), CHONG CHEN¹, HONGBING SHI³, AND ZHILEI YAO¹, (Senior Member, IEEE)

¹School of Electrical Engineering, Yancheng Institute of Technology, Yancheng 224051, China

²Center for Advanced Life Cycle Engineering, University of Maryland at College Park, College Park, MD 20740, USA

³State Grid Yancheng Power Supply Company, Yancheng 224005, China

Corresponding author: Simin Peng (psm2016@umd.edu)

This work was supported in part by the National Natural Science Foundation of China under Grant 51507150, in part by the Natural Science Foundation of Jiangsu Province of China under Grant BK20150430, in part by the Project of Natural Science Foundation of Higher Education Institutions of Jiangsu Province under Grant 15KJB480004, in part by the Science and Technology Project of State Grid of China under Grant J2017128, and in part by the Qing Lan Project of Jiangsu Province under Grant 2016-15.

ABSTRACT Since the noise statistics of large-scale battery energy storage systems (BESSs) are often unknown or inaccurate in actual applications, the estimation precision of state of charge (SOC) of BESSs using extended Kalman filter (EKF) or unscented Kalman filter (UKF) is usually inaccurate or even divergent. To resolve this problem, a method based on adaptive UKF (AUKF) with a noise statistics estimator is proposed to estimate accurately SOC of BESSs. The noise statistics estimator based on the modified Sage-Husa maximum posterior is aimed to estimate adaptively the mean and error covariance of measurement and system process noises online for the AUKF when the prior noise statistics are unknown or inaccurate. The accuracy and adaptation of the proposed method is validated by the comparison with the UKF and EKF under different real-time conditions. The comparison shows that the proposed method can achieve better SOC estimation accuracy when the noise statistics of BESSs are unknown or inaccurate.

INDEX TERMS Adaptive unscented Kalman filter, battery energy storage systems, noise statistics estimator, state of charge.

I. INTRODUCTION

With the rapid development of computer technique and power electronic technology, renewable energy sources such as photovoltaic and wind power are considered as a good solution for the looming depletion of fossil fuels and environmental pollution. However, the voltage and frequency of the power feeder will be degraded when high penetration of the renewable energy sources is integrated to the grid due to the inherent disadvantages of intermittence and randomness [1]. As a promising alternative method, battery energy storage systems (BESSs) is widely used to smooth the fluctuation of active power and reactive power and maintain the voltage and frequency of the power feeder at a desired level for the integration of renewable energy sources [2]. The BESSs is mainly composed of a power conversion system, a battery system, and a battery management system. As one of the most essential parts in BESSs, the battery system, which consists of thousands of cells, greatly impacts its performance. For the secure and safe operation of the BESSs, it is essential to

accurately estimate the battery system capacity. As an key indicator for the battery system, state of charge (SOC) is used to illustrate the battery system capacity because the battery system is an electrochemical system with strong nonlinearity and it is very difficult to directly measure its capacity by sensors [3]. Moreover, many serious adverse consequences will occur due to the incorrect or inaccurate SOC of the battery system. For example, a battery system with an incorrect SOC can be overcharged or overdischarged, which can damage the batteries and shorten the lifecycles, or even cause fire and/or explosion. Besides, the effect of control and optimization of a controller based on the fault SOC will also be degraded in the BESSs [4].

Many methods have been presented in previous literature to improve the SOC estimation accuracy of batteries. The coulomb counting (ampere-hour counting) method integrates the currents flowing into and out of the batteries over time to estimate SOC. However, this method's estimation is not accurate enough because it needs prior knowledge of the

initial SOC and suffers from the measurement errors and accumulated errors [5]. The open circuit voltage (OCV) method is a widely used approach, but needs a long rest time to measure the terminal voltage and small variations of lithium-ion batteries around their nominal voltage, thus degrading the estimation accuracy [6]. The electrochemical impedance spectroscopy method is too complicated to estimate SOC for online applications [7]. Intelligent algorithms, such as artificial neural networks [8], sliding mode observers [9], and particle filters [10] have been studied recently. These methods can accurately estimate the SOC for nonlinear systems, but are difficult to use online due to the enormous amount of samples and computational complexity.

Recently, the extended Kalman filter (EKF) has attracted increasing attention and becomes one of the most popular methods to estimate the battery SOC even when the initial SOC is unknown [11]. The EKF based on nonlinear state space battery model requires the linearized approximations of nonlinear function using first-order or second-order terms of Taylor's formula and the computation of Jacobian matrix to estimate the SOC, which degrades the SOC estimation accuracy. To overcome these drawbacks, a regular unscented Kalman filter (UKF) is presented as a sigma-point KF method to estimate the SOC [12]. The UKF based on unscented transform not only does not require the calculation of Jacobian matrix, but has a higher order of accuracy in the noise statistics estimation than the EKF, such as the mean and error covariance of the state vector of the battery system. However, it is assumed that the prior variables of the system process and measurement noise are known both in the UKF and the EKF. In practice, these prior noise statistics are often unknown or inaccurate and can result in remarkable errors and easily lead to the instability or even divergence of the UKF and EKF [13].

Much effort has been put into improving the SOC estimation accuracy of batteries with inaccurate prior noise statistics. A new SOC estimation method based on square root unscented Kalman filter (SRUKF) is presented [14]. The method requires one weighting parameter and improves the accuracy of state covariance. Zhang *et al.* [15] proposed a novel adaptive H infinity filter (AHIF) which applies a covariance matching technique to realize the adaptive estimation of the error covariance values. Due to the existing steady-state estimation errors of the covariance matching method, the SOC estimation accuracy of the batteries in BESSs is still degraded and instability using the AHIF and the SRUKF [16]. A novel method based on the Sage-Husa maximum posterior (SHMP) is employed to obtain the mean and error covariance of the system process noise and the measurement noise separately [17]. However, the SHMP will be incorrect or even divergent due to the noise covariance matrix may not be positive definite in the high-order system sometimes [18]. An adaptive UKF (AUKF) method using the output measured data in the UKF context is presented to implement the adaptive adjustment of noise covariance [19]. The SOC estimation results using the AUKF shows more

accuracy in comparison with the UKF and EKF approaches. In this paper, a method based on AUKF with a noise statistics estimator is developed to estimate the SOC of BESSs. The noise statistics estimator is based on a modified Sage-Husa maximum posterior and is aimed to estimate adaptively the mean and error covariance of the measurement and process noises online for the AUKF when the prior noise statistics are unknown or inaccurate.

The rest of the paper is organized as follows. In Section II, the operating principles of the BESSs and equivalent circuit model (ECM) of the battery system are described. The SOC estimation method based on AUKF with a noise statistics estimator is presented in Section III. Simulation and experimental results used to validate the proposed method are discussed in Section IV. Finally, Section V concludes the paper.

II. OPERATING PRINCIPLES OF THE BESSs AND THE BATTERY SYSTEM MODEL

As a promising method to alleviate traditional power grid problems, such as the depletion of fossil fuels and environmental pollution, renewable energy sources have attracted more and more attention. Due to the inherent natures of randomness and intermittence, high penetration of the renewable energy sources is frequently combined with the BESSs to improve system performance when those sources are integrated to the grid. The BESSs not only can keep the balance of active power and reactive power of the grid, but can maintain the voltage and frequency of the power feeder at an acceptable level.

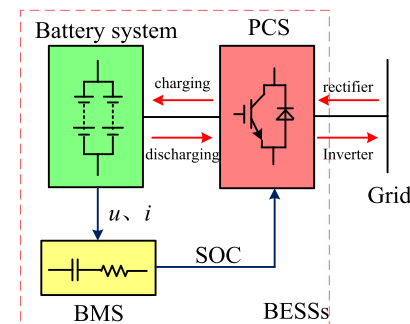


FIGURE 1. Structure diagram of the BESSs.

A. OPERATING PRINCIPLES OF THE BESSs

In Fig.1, a simple scheme of the studied BESSs is shown, which consists of three main parts: power conversion system (PCS), battery system, and battery management system (BMS). The PCS consists of a three-phase full bridge converter that couples the battery system to the grid, which can be used to as a rectifier in the charging process and as an inverter in the discharging process for the battery system. Moreover, the PCS combined with the battery system can maintain the voltage and frequency of the power feeder via regulating the active power and reactive power output of the battery system. The battery system is composed of thousands of cells which are connected in parallel and/or series to meet

the capacity requirements of the BESSs. The BMS is usually applied to measure the battery system performance parameters, such as voltages, currents, and temperatures, and so on. It is also used to monitor the states of the battery system and communicate with the PCS via the states, such as SOC, state of health (SOH), and so on.

In general, for the BESSs, its capacity of power and energy that can be exchanged with the grid is subjected to the state of the battery system. That is to say, the SOC of the battery system is a key indicator, which directly determines the operating mode and the exchanged capacity of the BESSs. For example, when the SOC is 1, which means the battery system is charged fully, the BESSs should stop charging the battery system to avoid damaging the batteries. Similarly, when the SOC is 0, which means the battery system is discharged fully, the BESSs should abandon the discharging mode because the battery system is empty. Therefore, it is essential to accurately obtain the SOC of the battery system for the secure and safe operation of the BESSs.

B. EQUIVALENT CIRCUIT MODEL OF THE BATTERY SYSTEM

In general, a battery system can supply high capacity when cells are connected in parallel and high voltage when cells are connected in series. In order to meet the requirement of high capacity and high voltage in the BESSs, the battery system is composed of thousands of cells connected in series and/or in parallel. Theoretically, any given battery system consisting of many cells in series and/or parallel may be simplified into a battery string in parallel connection or a battery string in series connection [20], [21]. The battery string can be further decomposed into a two-cell series or parallel connection. In reverse, a two-cell in parallel or series connection can be extended to a battery system consisting of thousands of cells in arbitrary connection. In this paper, the structure diagram of the researched battery system is shown as Fig. 2. It is assumed that the battery system consists of m battery strings (BSs) connected in parallel and each BSs is composed of n cells connected in series.

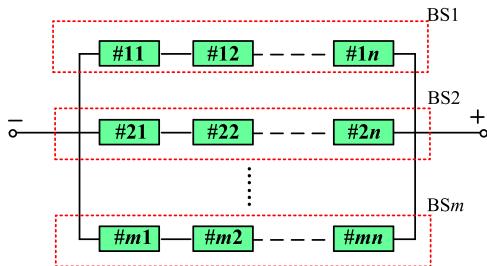


FIGURE 2. Structure diagram of the battery system.

As shown in Fig.2, the current through the corresponding BSs in series connection is equivalent to the current through each cell; the voltage of the BSs can be calculated in the sum of all voltage of each cell. Similarly, the current through the battery system of parallel connection is the sum of all current of each BSs; the voltage of the battery system is equivalent to the voltage of each BSs.

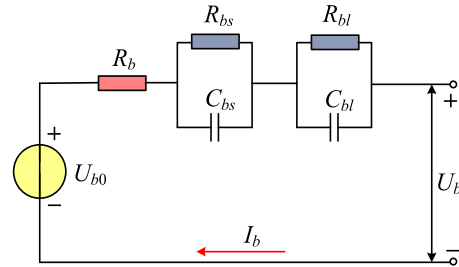


FIGURE 3. Equivalent circuit model of the battery system.

A state-of-the-art review of battery models can be found in [22]. In this paper, an equivalent circuit model (ECM) based on two-order RC circuit is shown in Fig. 3 [11]. The circuit is comprised of a controlled voltage source (U_{b0}), a resistor (R_b), and two resistor-capacitor (RC) networks in series. The U_{b0} illustrates the open circuit voltage of the battery system and its value changes with the SOC. The R_b represents the battery internal resistance variation during the discharging/charging process. The two RC networks model the relaxation effects of discharging/charging process of the battery. The R_{bs} and C_{bs} and the R_{bl} and C_{bl} are used to present the short-term transient response and long-term transient response of the battery, respectively. The I_b and U_b show the current and the terminal voltage of the battery system, respectively.

In general, the battery system performance in terms of internal resistance, terminal voltage, and current is sensitive to many factors, such as the inconsistent quality of cells, the connection mode of cells, the variable capacity of cells at different discharge current rate, and so on [21]. That is to say, the performance parameters of battery system shown in Fig.3 are sensitive to those above factors, which mainly derive from the performance parameters of cell-to-cell variation. In practice, the cells that are used to construct the battery system usually are selected by a screening process for the stable configuration of the battery system and in order to ensure the safety and management of the battery system [23]. In [23], [24], an approach based on a screening process is proposed to illustrate the relation between the performance parameters of each cell and the performance parameters of the battery system. The relation can be presented as follows [23], [24]

$$\left\{ \begin{array}{l} U_{b0}(t) = nU_0(t) \\ R_b(t) = \frac{n}{m}R(t) \\ R_{bl}(t) = \frac{n}{m}R_l(t) \\ R_{bs}(t) = \frac{n}{m}R_s(t) \\ C_{bl}(t) = \frac{n}{m}C_l(t) \\ C_{bs}(t) = \frac{n}{m}C_s(t) \\ I_b(t) = mI(t) \end{array} \right. \quad (1)$$

where U_0 is the open circuit voltage of cell, R is the internal resistance of cell, R_s and C_s are used to present the short-term transient response of cell, R_l and C_l illustrate the long-term transient response of cell, and I denotes the current through the cell in series. In general, the static relationships between U_0 , R_s , C_s , R_l , C_l , R and the SOC are intrinsically nonlinear. To obtain those nonlinear functions, many of tests are conducted using lithium-ion batteries. Based on the experimental data, the least squares error curve-fitting method is used to describe respectively the nonlinear relationships between the U_0 , R_s , C_s , R_l , C_l , R and the SOC as follows [25]

$$\begin{cases} U_0(t) = a_0 e^{-a_1 \text{SOC}(t)} + a_2 + a_3 \text{SOC}(t) \\ \quad - a_4 \text{SOC}^2(t) + a_5 \text{SOC}^3(t) \\ R(t) = b_0 e^{-b_1 \text{SOC}(t)} + b_2 + b_3 \text{SOC}(t) \\ \quad - b_4 \text{SOC}^2(t) + b_5 \text{SOC}^3(t) \\ R_s(t) = c_0 e^{-c_1 \text{SOC}(t)} + c_2 \\ C_s(t) = d_0 e^{-d_1 \text{SOC}(t)} + d_2 \\ R_l(t) = e_0 e^{-e_1 \text{SOC}(t)} + e_2 \\ C_l(t) = f_0 e^{-f_1 \text{SOC}(t)} + f_2 \\ \text{SOC}(t) = \text{SOC}_0 - \frac{\int \eta I(t) dt}{C_0} \end{cases} \quad (2)$$

where t denotes the discharging or charging time, SOC_0 is the initial value of SOC, η denotes the coulomb efficiency, C_0 shows the nominal capacity, the coefficients, namely, $a_0 \sim a_5$, $b_0 \sim b_5$, $c_0 \sim c_2$, $d_0 \sim d_2$, $e_0 \sim e_2$, $f_0 \sim f_2$ can be identified by the least squares error curve-fitting method based on experimental data, which have been described in detail in [26]. The coefficients of cell performance parameters in the paper are shown in Table 1.

TABLE 1. The coefficients of cell performance parameters.

	Normal voltage	3.7V	Battery capacity	860mAh
a_0	-0.915	a_1	40.867	a_2
a_3	0.537	a_4	0.499	a_5
b_0	0.1463	b_1	30.27	b_2
b_3	0.0584	b_4	0.1747	b_5
c_0	0.1063	c_1	62.49	c_2
d_0	-200	d_1	138	d_2
e_0	0.0712	e_1	61.4	e_2
f_0	-3083	f_1	180	f_2

Besides, the relation between the terminal voltage U_b of the battery system and the battery system current I_b can be expressed as shown in Fig.3

$$U_b(t) = U_{b0}(t) - I_b(t) \times [R_b(t) + \frac{R_{bs}(t)}{1+R_{bs}(t)jC_{bs}} + \frac{R_{bl}(t)}{1+R_{bl}(t)jC_{bl}(t)}] \quad (3)$$

C. STATE SPACE EQUATIONS FOR THE BATTERY SYSTEM MODEL

For further analysis, we chose the SOC, the voltage of the capacitor $C_{bs}(U_{bs})$, and the voltage of the capacitor $C_{bl}(U_{bl})$ as system state variables. The I_b was selected as input variables of the system. Based on the battery ECM as shown in Fig.3, the state space equation in discrete time can be expressed as

$$\begin{bmatrix} \text{SOC}_{k+1} \\ U_{bs,k+1} \\ U_{bl,k+1} \end{bmatrix} = \begin{bmatrix} 1 & 0 & 0 \\ 0 & \exp(-\Delta t/\tau_1) & 0 \\ 0 & 0 & \exp(-\Delta t/\tau_2) \end{bmatrix} \times \begin{bmatrix} \text{SOC}_k \\ U_{bs,k} \\ U_{bl,k} \end{bmatrix} + \begin{bmatrix} -\eta \Delta t / C_0 \\ R_{bs}[1 - \exp(-\Delta t/\tau_1)] \\ R_{bl}[1 - \exp(-\Delta t/\tau_2)] \end{bmatrix} \times I_{b,k} + w_k \quad (4)$$

where the w_k is the system process noise at k step, the τ_1 and τ_2 are time parameters and can be obtained as

$$\tau_1 = R_{bs} C_{bs} \quad (5)$$

$$\tau_2 = R_{bl} C_{bl} \quad (6)$$

Similarly, according to the circuit shown in Fig.3, the output equation in discrete time can be written as

$$[U_{b,k+1}] = U_{b0,k+1} - R_{b,k+1} I_{b,k+1} - U_{bs,k+1} - U_{bl,k+1} + v_k \quad (7)$$

where v_k is the measurement noise at k step.

III. THE PROPOSED AUKF WITH A NOISE STATISTICS ESTIMATOR

Based on the analysis previously stated, the proposed AUKF with a noise statistics estimator is demonstrated in this section. The noise statistics estimator is used to estimate the mean and error covariance of measurement and process noises, which are regarded as the input of AUKF to estimate the SOC.

A. STANDARD UKF

For a discrete time nonlinear system, the system state and measurement equation can be expressed as [19]

$$\begin{cases} x_k = f(x_{k-1}, u_k) + w_k \\ y_k = g(x_k, u_k) + v_k \end{cases} \quad (8)$$

where x_k and y_k denote, respectively, the system state vector and the system measurement vector. u_k denotes the system input vector. f and g denote, respectively, the nonlinear process and measurement models. w_k and v_k denote the system process noise and the measurement noise separately, which are both uncorrelated zero-mean Gaussian white sequences. The detailed steps of the UKF can be summarized as follows:

- 1) Initialize the mean (\bar{x}_0) and the covariance (P_0) of the initial system state x_0

$$\begin{cases} \bar{x}_0 = E(x_0) \\ P_0 = E[(x_0 - \bar{x}_0)(x_0 - \bar{x}_0)^T] \end{cases} \quad (9)$$

where $E(\cdot)$ is expectation mean value.

- 2) Calculate sigma points at $k - 1$ step

$$\begin{cases} x_{0,k-1} = \hat{x}_{k-1} \\ x_{i,k-1} = \hat{x}_{k-1} + (\sqrt{(n+\lambda)P_{k-1}})_i, & i = 1, 2, \dots, n \\ x_{i,k-1} = \hat{x}_{k-1} - (\sqrt{(n+\lambda)P_{k-1}})_i, & i = n+1, n+2, \dots, 2n \end{cases} \quad (10)$$

where n is the dimension of the state variable, λ is a scale which can be expressed as

$$\lambda = \alpha^2(n + h) - n \quad (11)$$

where α is a scaling parameter which determines the spread of the sigma point around \hat{x} , its range is $0 \sim 1$, here we assume $\alpha = 1$; h is a scaling parameter, usually we let $h = 0$.

Weighted coefficients are separately

$$\begin{cases} \omega_0^m = \frac{\lambda}{(n + \lambda)} \\ \omega_0^c = \frac{\lambda}{(n + \lambda)} + (1 + \beta - \alpha^2) \\ \omega_i^m = \omega_i^c = \frac{1}{2(n + \lambda)}, & i = 1, 2, \dots, 2n, \end{cases} \quad (12)$$

where ω^m, ω^c are the weight factors respectively; β is a parameter which restrains error caused by the higher order terms, here we assume $\beta = 2$.

- 3) Time update for the mean and covariance of system states at time instant $k | k - 1$

- a. Update the sample point

$$x_{i,k|k-1} = f(x_{i,k-1}, u_k), \quad i = 0, 1, \dots, 2n \quad (13)$$

- b. Estimate the system state

$$\hat{x}_{k|k-1} = \sum_{i=0}^{2n} \omega_i^m f(x_{i,k-1}, u_k) + q_k \quad (14)$$

where q_k is the mean of system process noise.

- c. Update the covariance of the estimated state

$$\begin{aligned} \bar{P}_{k|k-1} = & \sum_{i=0}^{2n} \omega_i^c (x_{i,k|k-1} - \hat{x}_{k|k-1}) \\ & \times (x_{i,k|k-1} - \hat{x}_{k|k-1})^T + Q_k \end{aligned} \quad (15)$$

where Q_k is the covariance of system process noise.

- 4) Measurement update

- a. Calculate measurement

$$\chi_{i,k|k-1} = g(x_{i,k-1}, u_k) \quad (16)$$

- b. Update measurement

$$\hat{y}_{k|k-1} = \sum_{i=0}^{2n} \omega_i^m g(x_{i,k-1}, u_k) + r_k \quad (17)$$

where r_k is the mean of measurement noise.

- 5) Calculate the UKF gain matrix L_k

$$L_k = \bar{P}_{xy,k} \bar{P}_{y,y}^{-1} \quad (18)$$

where

$$\begin{cases} \bar{P}_{y,k} = \sum_{i=0}^{2n} \omega_i^c (\chi_{i,k|k-1} - \hat{y}_{k|k-1}) \\ \times (\chi_{i,k|k-1} - \hat{y}_{k|k-1})^T + R_k \\ \bar{P}_{xy,k} = \sum_{i=0}^{2n} \omega_i^c (x_{i,k|k-1} - \hat{x}_{k|k-1}) \\ \times (\chi_{i,k|k-1} - \hat{y}_{k|k-1})^T, \end{cases}$$

where R_k is the covariance of measurement noise.

- 6) Measurement correction

- a. Update the estimated state

$$\hat{x}_k = \hat{x}_{k|k-1} + L_k (y_k - \hat{y}_{k|k-1}) \quad (19)$$

- b. Update the propagated covariance

$$P_k = \bar{P}_{k|k-1} - L_k \bar{P}_{y,y} L_k^T \quad (20)$$

B. NOISE STATISTICAL ESTIMATOR

For the SOC estimation of batteries, the estimation accuracy is extremely correct using the UKF and SRUKF when the prior noise statistic characteristics are given. In practice, the mean and covariance of process noise and measurement noise such as q_k in (14), Q_k in (15), r_k in (17) and R_k in (18) are frequently unknown or incorrect; the UKF experiences limitation such as the incorrectness or even instability due to the uncertain noise statistics. To overcome these shortcomings, methods based on covariance matching technique are proposed in the SOC estimation [15], [27]. A novel AUKF method based on the output voltage of battery model is proposed in [19]. Among these approaches, both the process noise covariance Q_k and the measurement noise R_k can be adaptively estimated accurately. However, it is still suffered from the inaccuracy and instability due to the uncertain mean of the process and measurement noise [18]. Recently, an estimator based on Sage-Husa maximum posterior has been widely used to attain the estimated value of q_k , Q_k , r_k and R_k respectively. The detailed calculations of these estimated noise statistics are obtained, respectively, as follows [17], [18], [28]

- 1) calculating estimated mean value of process noise

$$\begin{aligned} \hat{q}_{k+1} = & (1 - d_{k+1}) \hat{q}_k + d_{k+1} \\ & \times [\hat{x}_{k+1} - \sum_{i=0}^{2n} \omega_i^m f(x_{i,k}, u_k)] \end{aligned} \quad (21)$$

where d_{k+1} is expressed as

$$d_{k+1} = \frac{1 - b}{1 - b^{k+1}} \quad (22)$$

where b is a forgetting factor, which is regularly set to 0.95.

2) calculating estimated covariance value of process noise

$$\begin{aligned}\hat{Q}_{k+1} = & (1 - d_{k+1})\hat{Q}_k + d_{k+1}[K_{k+1}e_{k+1}e_{k+1}^T K_{k+1}^T \\ & + P_{k+1} - \sum_{i=0}^{2n} \omega_i^c(x_{i,k+1/k} - \hat{x}_{k+1/k}) \\ & \times (x_{i,k+1/k} - \hat{x}_{k+1/k})^T]\end{aligned}\quad (23)$$

where e_{k+1} is a error term, which is expressed as

$$e_k = y_k - \hat{y}_k \quad (24)$$

3) calculating estimated mean value of measurement noise

$$\begin{aligned}\hat{r}_{k+1} = & (1 - d_{k+1})\hat{r}_k + d_{k+1} \\ & \times [y_{k+1} - \sum_{i=0}^{2n} \omega_i^m g(x_{i,k+1/k}, u_k)]\end{aligned}\quad (25)$$

4) calculating estimated covariance value of measurement noise

$$\begin{aligned}\hat{R}_{k+1} = & (1 - d_{k+1})\hat{R}_k + d_{k+1}[e_{k+1}e_{k+1}^T \\ & - \sum_{i=0}^{2n} \omega_i^c(x_{i,k+1/k} - \hat{y}_{k+1/k}) \\ & \times (\chi_{i,k+1/k} - \hat{y}_{k+1/k})^T]\end{aligned}\quad (26)$$

In contrast to the UKF and the methods based on covariance matching method, the \hat{q}_k , \hat{Q}_k , \hat{r}_k and \hat{R}_k can be obtained online by the noise estimator based on the Sage-Husa maximum posterior. However, the stability and estimate accuracy of the noise estimator are sensitive to its complex calculation and the convergence of the covariance of process and measurement noise [13]. For a stable system, it is obviously known that the estimated state and measurement covariance will converge to a small value or even to zero when the filtering process begin converging. Then, we can attain theoretically

$$\sum_{i=0}^{2n} \omega_i^c(x_{i,k+1/k} - \hat{x}_{k+1/k})(x_{i,k+1/k} - \hat{x}_{k+1/k})^T \approx 0 \quad (27)$$

$$\sum_{i=0}^{2n} \omega_i^c(\chi_{i,k+1/k} - \hat{y}_{k+1/k})(\chi_{i,k+1/k} - \hat{y}_{k+1/k})^T \approx 0 \quad (28)$$

Substituted formula (27) with formula (23), and formula (28) with formula (26), we can obtain a modified noise statistics estimator, which is expressed as follows

$$\left\{ \begin{array}{l} \hat{q}_{k+1} = (1 - d_{k+1})\hat{q}_k + d_{k+1}[\hat{x}_{k+1} - \sum_{i=0}^{2n} \omega_i^m f(x_{i,k}, u_k)] \\ \hat{Q}_{k+1} = (1 - d_{k+1})\hat{Q}_k + d_{k+1}[K_{k+1}e_{k+1}e_{k+1}^T K_{k+1}^T + P_{k+1}] \\ \hat{r}_{k+1} = (1 - d_{k+1})\hat{r}_k + d_{k+1}[y_{k+1} - \sum_{i=0}^{2n} \omega_i^m g(x_{i,k+1/k}, u_k)] \\ \hat{R}_{k+1} = (1 - d_{k+1})\hat{R}_k + d_{k+1}e_{k+1}e_{k+1}^T \end{array} \right. \quad (29)$$

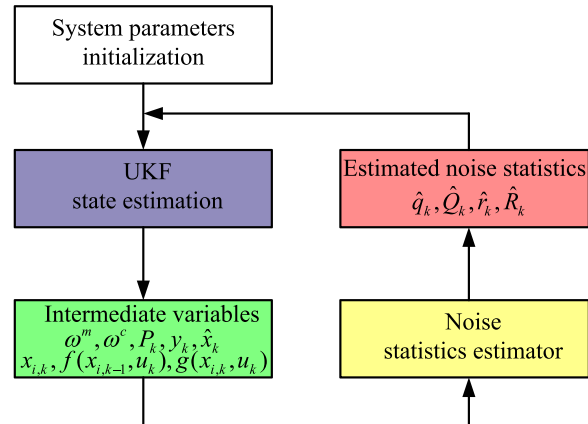


FIGURE 4. Implementation flowchart of AUKF with noise statistical estimator.

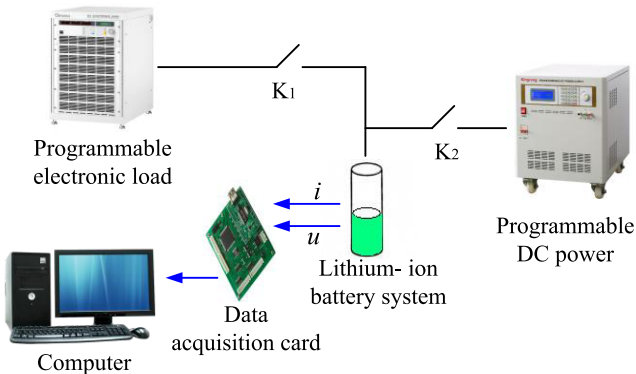
C. SOC ESTIMATION BASED ON AUKF

To estimate the SOC of batteries online, the q_k , Q_k , r_k and R_k of the UKF are substituted by the \hat{q}_k , \hat{Q}_k , \hat{r}_k and \hat{R}_k respectively which are adaptively estimated using the noise statistics estimator based on the modified Sage-Husa maximum posterior. When the system state \bar{x} is estimated in the iterative process using the standard UKF, the SOC of battery system can be estimated finally. Therefore, an adaptive SOC estimation based on the AUKF with a noise statistics estimator can be established. The implementation flowchart of the proposed AUKF is shown in Fig. 4.

As shown in Fig. 4, some system parameters are initialized firstly, including the initial values of SOC_0 , α , β , n , and the mean and covariance of process noise and measurement noise (\hat{q}_0 , \hat{Q}_0 , \hat{r}_0 and \hat{R}_0). In this paper, the value of α is set to 1 and β is set to 2 and n is set to 3. In theory, the values of SOC_0 , \hat{q}_0 , \hat{Q}_0 , \hat{r}_0 and \hat{R}_0 which can be set randomly are initialized in details in section IV according to the different experimental conditions. Afterward, the intermediate variables at the k th time (ω^m , ω^c , P_k , \hat{x}_k , $x_{i,k}$, $f(x_{i,k-1}, u_k)$, $g(x_{i,k}, u_k)$, y_k) can be calculated using the estimated noise statistics at the $(k-1)$ th time (\hat{q}_{k-1} , \hat{Q}_{k-1} , \hat{r}_{k-1} and \hat{R}_{k-1}) from (31) to (20) in the UKF iterative process. The intermediate variables are used by the noise statistics estimator to attain the estimated noise statistics at the k th time (\hat{q}_k , \hat{Q}_k , \hat{r}_k and \hat{R}_k), which are propagated in the next UKF iteration. In this way, the proposed AUKF recursive process is constructed base on the UKF and a noise statistics estimator, and thus the SOC can be estimated by the AUKF.

IV. SIMULATION AND EXPERIMENTAL RESULTS

To further evaluate the performance of the proposed AUKF with a noise statistics estimator, some comparisons of simulation results with the experimental data are conducted. An experimental test plat is set up as shown in Fig. 5, including a 3×3 lithium-ion battery system (3 battery strings in parallel which is composed of 3 cells in series), a programmable DC power, a data acquisition card, a computer,

**FIGURE 5.** General diagram of the experiment platform.**TABLE 2.** Cell specification.

Type	PL 383562
National voltage (V)	3.7
National capacity (mAh)	860
Upper cut-off voltage (V)	4.2
Lower cut-off voltage (V)	3

and a programmable electronic load. The programmable DC power supplies the lithium-ion batteries with DC power in charging process. The data acquisition card is used to record the current and terminal voltage of the battery and send the data to the computer. The computer is used to estimate the SOC using the AUKF and other SOC estimation methods with the measured data from the data acquisition card. The programmable electronic load connected to the lithium-ion batteries through the switcher K₁ is used to simulate various loads in discharging process. The key specification of each cell is listed in Table 2.

To validate the efficiency and accuracy of the proposed AUKF method with a noise statistical estimator, the corresponding SOC estimations using the AUKF and UKF are evaluated when process statistical noises are unknown and measurement statistical noises are not given respectively. Moreover, a comparison of SOC estimation results between the AUKF, EKF, and UKF is conducted to validate the better performance of the proposed method.

A. SOC ESTIMATION WITH UNKNOWN PROCESS STATISTICAL NOISES

Firstly, we assume the mean and covariance of measurement statistical noises are given ($r_0 = 0.8$, $R_0 = 0.03$) and the process noise statistics are selected randomly. The initial SOC of the AUKF and UKF is uniformly set as 0.8, and the initial value of the measured SOC namely SOC₀ is set as 0.9. To evaluate the performance of SOC estimation using the AUKF and UKF with different process statistical noises, four groups of incorrect initial values of the process statistical noises are selected randomly in Table 3.

Fig. 6 shows the SOC estimation results comparison using UKF versus AUKF with different random process noises

TABLE 3. The given process statistics.

	q_0	Q_0
UKF1	0.002	0.0005
UKF2	0.18	0.02
AUKF1	0.002	0.0005
AUKF2	0.18	0.02

TABLE 4. The given measurement statistics.

	r_0	R_0
UKF1	0.002	0.03
UKF2	0.2	0.3
AUKF1	0.002	0.03
AUKF2	0.2	0.3

under constant discharging current (1C). Fig. 6 (a) shows the constant discharging current profiles at 1C (2.4A). The SOC estimation and reference results and the corresponding estimation absolute errors are shown in Fig. 6 (b) and (c) separately. From the results, it is clear that the AUKF method illustrates a better performance of the stronger noise filtering ability and higher SOC estimation accuracy. As shown in Fig. 6 (b), the SOC estimation using the AUKF1 and AUKF2 method not only can rapidly converge to the measured value within 20 s, but maintain a good magnitude consistency. Conversely, the magnitude of the SOC using the UKF1 is obviously great different from the magnitude using the UKF2 after convergence. Moreover, it can be illustrated in Fig. 6 (c) that the AUKF method provide more stable and accurate SOC estimation than the UKF, which means the AUKF can estimate the SOC more accurately and shows higher robustness when the process statistical noises are unknown.

B. SOC ESTIMATION WITH UNKNOWN MEASUREMENT STATISTICAL NOISES

To evaluate the performance of the proposed method when the measurement noises are not accuracy or known, we assume the process statistical noises are clearly known, which are set as ($q_0 = 0.8$, $Q_0 = 0.03$). Four groups of initial values of the measurement statistical noises are also selected. Table 4 shows the selected measurement noises.

The SOC estimation results comparison using UKF and AUKF at different random measurement noises is shown in Fig. 7. Fig. 7 (a) shows the SOC estimation and reference results. It can be seen that both the AUKF1 and AUKF2 can quickly consistently track the referent SOC₀ after convergence in step, which illustrates a strong noise-filtering robustness of the proposed AUKF. Due to without the noise estimator which contributes to filter noise statistics, there is a great difference between the UKF1 and UKF2 in the whole discharging process. A comparison of SOC estimation absolute errors is shown in Fig. 7 (b). It is noted that the variation of the SOC estimation errors using the AUKF is smaller than the UKF1 and UKF2.

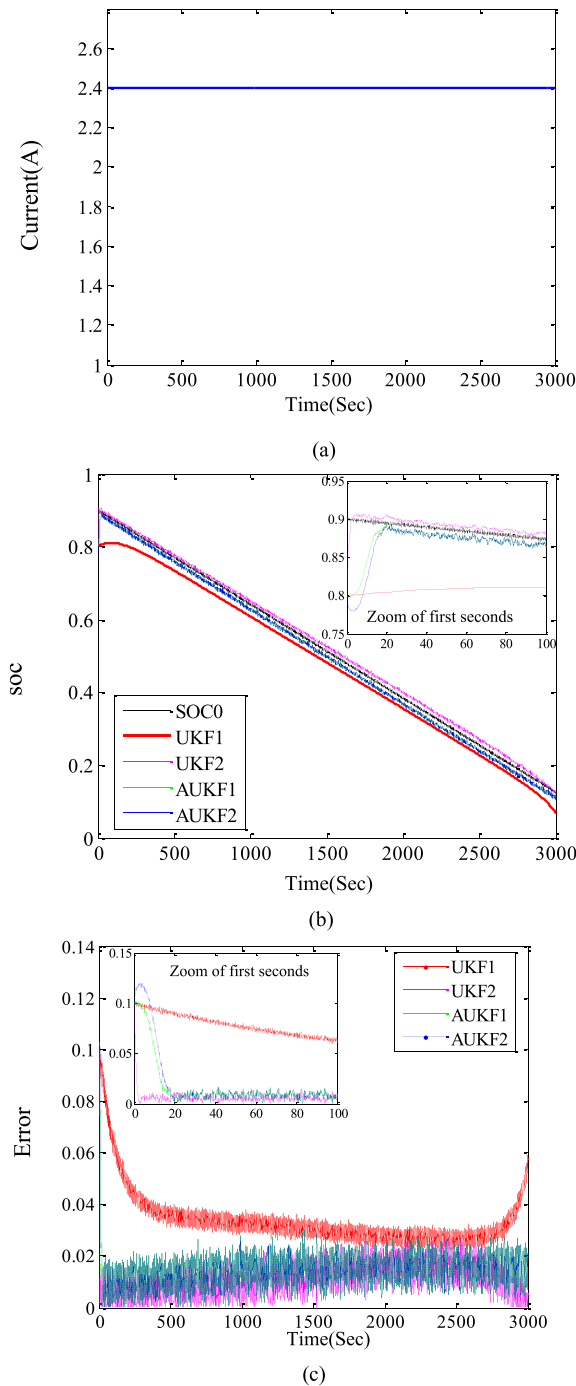


FIGURE 6. SOC estimation results using UKF versus AUKF at different process noises: (a) Current profiles. (b) SOC estimation and reference results. (c) SOC estimation errors.

C. COMPARISON

To further validate the accuracy and adaptation of the proposed AUKF, some comparisons of SOC estimation are carried out in this section. Fig. 8 shows the SOC estimation comparison of the AUKF, UKF, and EKF in the case of dynamic discharging current. Fig. 8 (a) shows the dynamic discharging current profiles. Each period is 137 s, the maximum output current is 5.55 A, and the average discharging

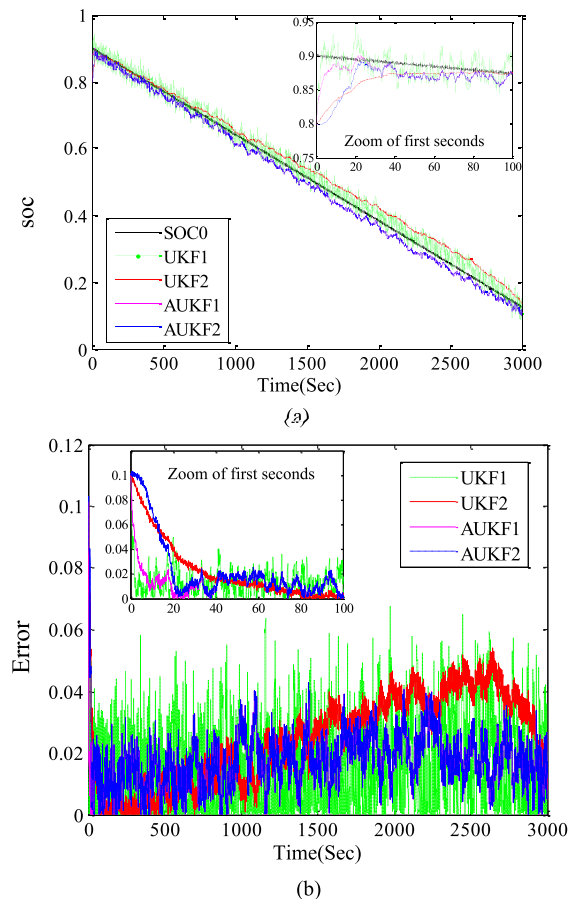


FIGURE 7. SOC estimation results using UKF versus AUKF at different measurement noises: (a) SOC estimation and reference results. (b) SOC estimation errors.

current is 1.92 A. Fig. 8 (b) and Fig. 8 (c) illustrate the SOC estimation and reference results and the corresponding estimation errors, respectively. It is seen that the EKF, UKF, and AUKF can be used to apply the SOC estimation with different estimation accuracy. Table 5 shows the comparisons of the root-mean square error (RMSE) and the mean absolute error (MAE) of the SOC in different method, respectively. The RMSE and MAE of the SOC are calculated as follows

$$\text{RMSE} = \sqrt{\frac{1}{n} \sum_{k=1}^n (x_i - \hat{x}_i)^2} \quad (30)$$

$$\text{MAE} = \frac{1}{n} \sum_{k=1}^n |x_i - \hat{x}_i| \quad (31)$$

From Table 5, it is clear that the AUKF has the lowest RMSE of 0.0163 and the lowest MAE of 0.0149, which means the AUKF can provide higher SOC estimation accuracy than the UKF and EKF under dynamic surroundings. Besides, being affected by the incorrect measurement noises and lack of the noise filtering ability, the SOC estimation using the EKF and UKF drift away from the reference SOC, especially to the EKF.

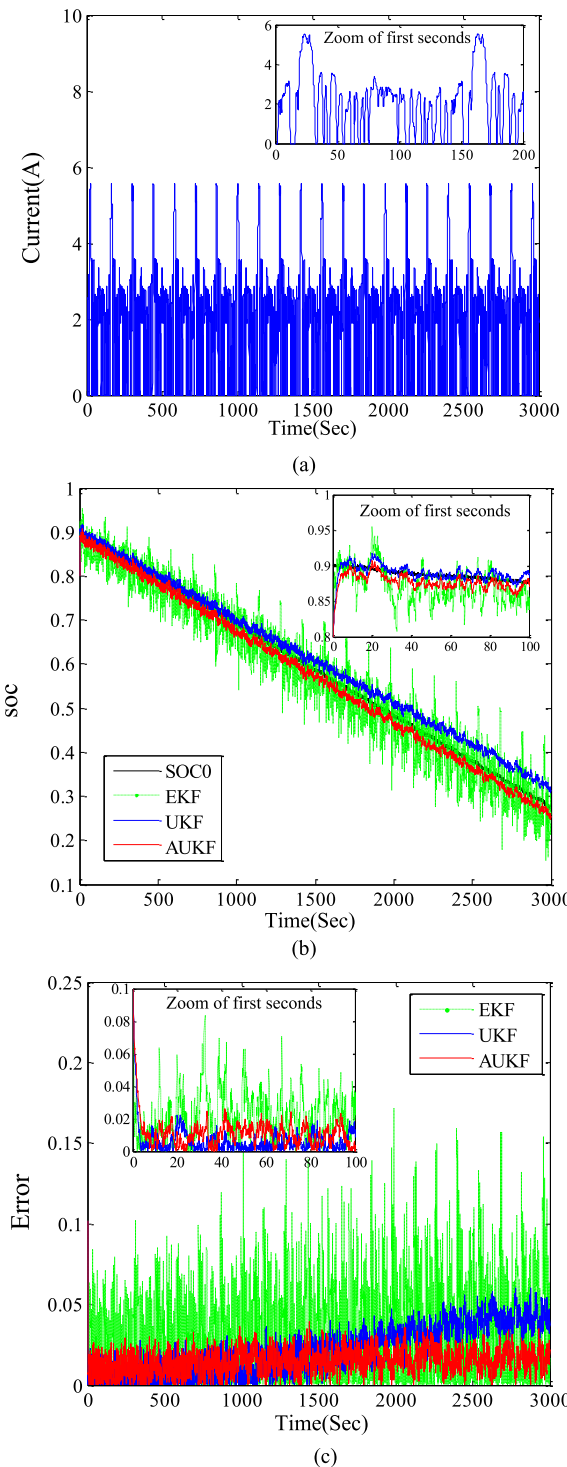


FIGURE 8. SOC estimation comparison using different methods:
(a) Current profiles. (b) SOC estimation and reference results. (c) SOC estimation errors.

To further validate the adaptation of the proposed method, a comparison of SOC estimation is performed when the initial SOC of AUKF is set as different value with different noise statistics. Table 6 shows the parameters of AUKF in detail. The initial SOCs of AUKFs are incorrectly set to 0.8, 0.85 and 0.95 separately, and two different groups of noise statistics are randomly selected for each same initial SOC of AUKF.

TABLE 5. Performance comparison.

Methods	RMSE	MAE
EKF	0.0379	0.0292
UKF	0.0258	0.0214
AUKF	0.0163	0.0149

TABLE 6. Parameters of AUKF.

SOC _{initial}	q_0	Q_0	r_0	R_0	Methods
0.8	0.01	0.03	0.002	0.0005	AUKF1
	0.1	0.3	0.2	0.01	AUKF2
0.85	0.03	0.1	0.005	0.001	AUKF3
	0.01	0.01	0.1	0.2	AUKF4
0.95	0.01	0.3	0.001	0.001	AUKF5
	0.001	0.01	0.1	0.2	AUKF6

TABLE 7. Performance comparison.

Methods	RMSE	MAE
AUKF1	0.0163	0.0149
AUKF2	0.0166	0.0150
AUKF3	0.0162	0.0148
AUKF4	0.0162	0.0149
AUKF5	0.0162	0.0148
AUKF6	0.0162	0.0149

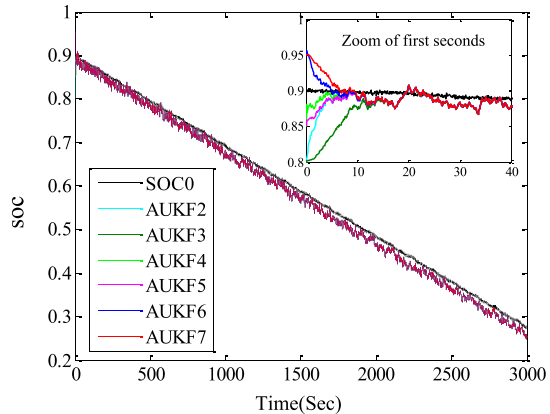


FIGURE 9. SOC estimation comparison when the initial SOC of the AUKF is set as different values with different noise statistics.

Fig. 9 shows SOC estimation results when the initial SOC of AUKF is set as different values with different noise statistics. Table 7 shows the performance comparison of SOC estimation. As shown in Fig. 9, in spite of the different incorrect initial SOC, the SOC estimation can rapidly converge to the given value within 20 s. Moreover, for the cases where the noise statistics are randomly given for the same initial SOC of AUKF, the SOC estimation can not only converge promptly, but track synchronously the measured SOC accurately. Take the case of the initial SOC of 0.8 as an example, as shown in Table 7, the RMSE of the SOC estimation of AUKF1 and AUKF2 are only 0.0163 and 0.0166, respectively, and the MAE of them are 0.0149 and 0.015, respectively, which indicates that the high estimation accuracy and strong adaptation of the developed method in spite of the incorrectness of the process and measurement statistical noises.

V. CONCLUSION

In this paper, based on a noise statistical estimator, a new SOC estimation approach using AUKF for BESSs has been developed. When the noise statistics of BESSs are unknown or are inaccurate, the developed method can be used to adaptively estimate the noise statistics in the iterative process of the AUKF. The simulation and experimental data of the proposed method have been compared with that of the UKF and EKF methods. The adaptation performance of SOC estimation for lithium-ion batteries in the BESSs using the proposed method is better, and the SOC accuracy is higher than the UKF and EKF under the surroundings of unknown process noise or unknown measurement noise. In addition, the developed method can be used to estimate SOC not only for batteries in the BESS, but also for battery packs, and for the EKF methods.

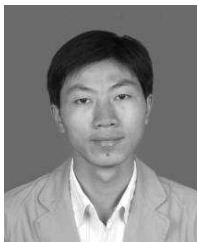
Nevertheless, the SOC estimation method does not consider the influence of cell inconsistency on the variation of battery system model parameters, which can affect the SOC estimation accuracy. For example, the battery model parameters, such as U_{b0} , R , R_s , C_s , R_l and C_l , will be improved considering the inconsistency of cells in multi-timescale, due to the variation of the above parameters are sensitive to the different timescale. Further work will be done to perfect the battery system model considering the inconsistency of cells, such as a multi-timescale battery system model.

REFERENCES

- [1] X. Liang, "Emerging power quality challenges due to integration of renewable energy sources," *IEEE Trans. Ind. Appl.*, vol. 53, no. 2, pp. 855–866, Mar. 2017.
- [2] R. Sebastián, "Battery energy storage for increasing stability and reliability of an isolated wind diesel power system," *IET Renew. Power. Generat.*, vol. 11, no. 2, pp. 296–303, Apr. 2017.
- [3] Z. Li, J. Huang, B. Y. Liaw, and J. Zhang, "On state-of-charge determination for lithium-ion batteries," *J. Power Sour.*, vol. 348, pp. 281–301, Apr. 2017.
- [4] F. Zheng, Y. Xing, J. Jiang, B. Sun, J. Kim, and M. Pecht, "Influence of different open circuit voltage tests on state of charge online estimation for lithium-ion batteries," *Appl. Energy*, vol. 183, pp. 513–525, Dec. 2016.
- [5] S. C. Huang, K. H. Tseng, J. W. Liang, C. L. Chang, and M. G. Pecht, "An online SOC and SOH estimation model for lithium-ion batteries," *Energies*, vol. 10, no. 4, pp. 512–529, Apr. 2017.
- [6] H. Sheng, J. Xiao, and P. Wang, "Lithium iron phosphate battery electric vehicle state-of-charge estimation based on evolutionary Gaussian mixture regression," *IEEE Trans. Ind. Electron.*, vol. 64, no. 1, pp. 544–551, Jan. 2017.
- [7] U. Westerhoff, T. Kroker, K. Kurbach, and M. Kurrrat, "Electrochemical impedance spectroscopy based estimation of the state of charge of lithium-ion batteries," *J. Energy Storage*, vol. 8, pp. 244–256, Nov. 2016.
- [8] W. He, N. Williard, C. Chen, and M. Pecht, "State of charge estimation for li-ion batteries using neural network modeling and unscented Kalman filter-based error cancellation," *Elect. Power Energy Syst.*, vol. 62, pp. 783–791, Jun. 2014.
- [9] Q. Chen, J. Jiang, H. Ruan, and C. Zhang, "Simply designed and universal sliding mode observer for the SOC estimation of lithium-ion batteries," *IET Power. Electron.*, vol. 10, no. 6, pp. 697–705, Apr. 2017.
- [10] X. Su, S. Wang, M. Pecht, L. Zhao, and Z. Ye, "Interacting multiple model particle filter for prognostics of lithium-ion batteries," *Microelectron. Rel.*, vol. 70, pp. 59–69, Mar. 2017.
- [11] Z. Chen, Y. Fu, and C. C. Mi, "State of charge estimation of lithium-ion batteries in electric drive vehicles using extended Kalman filtering," *IEEE Trans. Veh. Technol.*, vol. 62, no. 3, pp. 1020–1030, Mar. 2013.
- [12] Y. Tian, B. Xia, W. Sun, Z. Xu, and W. Zheng, "A modified model based state of charge estimation of power lithium-ion batteries using unscented Kalman filter," *J. Power Sources*, vol. 270, pp. 619–626, Dec. 2014.
- [13] J. Meng, G. Luo, and F. Gao, "Lithium polymer battery state-of-charge estimation based on adaptive unscented Kalman filter and support vector machine," *IEEE Trans. Power Electron.*, vol. 31, no. 3, pp. 2226–2238, Mar. 2016.
- [14] H. G. Narm and M. Charkgard, "Lithium-ion battery state of charge estimation based on square-root unscented Kalman filter," *IET Power. Electron.*, vol. 6, no. 9, pp. 1833–1841, Nov. 2013.
- [15] Y. Zhang, R. Xiong, H. He, and W. Shen, "Lithium-ion battery pack state of charge and atate of energy estimation algorithms using a hardware-in-the-loop validation," *IEEE Trans. Power Electron.*, vol. 32, no. 6, pp. 4421–4431, Jun. 2017.
- [16] W. Lu, L. G. Chun, Q. X. Wei, and W. Z. Long, "An adaptive UKF algorithm based on maximum likelihood principle and expectation maximization algorithm," *Acta Autom. Sinica*, vol. 38, no. 7, pp. 1200–1210, Jul. 2012.
- [17] A. P. Sage and G. W. Husa, "Adaptive filtering with unknown prior statistics," in *Proc. Joint Autom. Control Conf.*, 1969, pp. 760–769.
- [18] S. Qingping and L. Rongke, "Weighted adaptive filtering algorithm for carrier tracking of deep space signal," *Chin. J. Aeronautics*, vol. 28, no. 4, pp. 1236–1244, Aug. 2015.
- [19] M. Partovibakhsh and G. Liu, "An adaptive unscented Kalman filtering approach for online estimation of model parameters and state-of-charge of lithium-ion batteries for autonomous mobile robots," *IEEE Trans. Control Syst. Technol.*, vol. 23, no. 1, pp. 357–363, Jan. 2015.
- [20] M. S. Wu, C.-Y. Lin, Y.-Y. Wang, C.-C. Wan, and C. R. Yang, "Numerical simulation for the discharge behaviors of batteries in series and/or parallel-connected battery pack," *Electrochim. Acta*, vol. 52, pp. 1349–1357, Nov. 2006.
- [21] J. Zhang, S. Ci, H. Sharif, and M. Alahmad, "Modeling discharge behavior of multicell battery," *IEEE Trans. Energy Convers.*, vol. 25, no. 4, pp. 1133–1141, Dec. 2010.
- [22] A. Fotouhi, D. J. Auger, K. Propp, S. Longo, and M. Wild, "A review on electric vehicle battery modelling: From lithium-ion toward lithium-sulphur," *Renew. Sustain. Energy Rev.*, vol. 56, pp. 1008–1021, Apr. 2016.
- [23] J. Kim, J. Shin, C. Chun, and B. H. Cho, "Stable configuration of a li-ion series battery pack based on a screening process for improved voltage SOC balancing," *IEEE Trans. Power Electron.*, vol. 27, no. 1, pp. 411–424, Jan. 2012.
- [24] J. Kim and B. H. L. Cho, "Screening process-based modeling of the multi-cell battery string in series and parallel connections for high accuracy state-of-charge estimation," *Energy*, vol. 57, pp. 581–599, Aug. 2013.
- [25] S. Peng, G. Shi, X. Cai, and R. Li, "Modeling and simulation of large capacity battery systems based on the equivalent circuit method," *CSEE*, vol. 33, no. 7, pp. 11–18, Mar. 2013.
- [26] M. Chen and G. A. Rincon-Mora, "Accurate electrical battery model capable of predicting runtime and I-V performance," *IEEE Trans. Energy Convers.*, vol. 21, no. 2, pp. 504–511, Jun. 2006.
- [27] F. Sun, X. Hu, Y. Zou, and S. Li, "Adaptive unscented Kalman filtering for state of charge estimation of a lithium-ion battery for electric vehicles," *Energy*, vol. 36, no. 5, pp. 3531–3540, 2011.
- [28] Z. Lin, X.-X. Wang, M. Sun, and C. Yan, "Adaptive UKF filtering algorithm based on maximum a posterior estimation and exponential weighting," *Acta Autom. Sinica*, vol. 36, no. 7, pp. 1007–1019, Jul. 2010.



SIMIN PENG (M'16) received the B.S degree in automation from Xiangtan University, Xiangtan, China, in 2003, and the Ph.D. degree in electrical engineering from Shanghai Jiao Tong University in 2013. He is currently with the School of Electrical Engineering, Yancheng Institute of Technology, China. His research interests include wind power, microgrid, battery energy storage system, and battery manage system. Since 2016, he has been a Visiting Scholar with CALCE, University of Maryland, College Park, USA, where he focuses on modeling and state of charge estimation of lithium-ion battery.

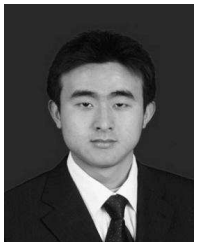


CHONG CHEN was born in Jiangsu, China, in 1982. He received the master's degree in electrical engineering from Jiangsu University in 2008. He is currently with the School of Electrical Engineering, Yancheng Institute of Technology, China. His current research interests include motion control and power electron application.



ZHILEI YAO (M'12–SM'15) was born in Jiangsu, China, in 1981. He received the B.S., M.S., and Ph.D. degrees from the Nanjing University of Aeronautics and Astronautics, Nanjing, China, in 2003, 2006, and 2012, respectively, all in electrical engineering.

He is currently with the School of Electrical Engineering, Yancheng Institute of Technology, Yancheng, China, where he is currently an Associate Professor. He holds 25 patents, and has authored or co-authored over 80 technical papers. His current research interests include dc–dc converters, inverters, and distributed power generation.



HONGBING SHI received the B.S. and M.S. degree in power system and automation from Southeast University, Nanjing, China, in 2004 and 2008, respectively.

He is currently an Associate Director of the Yancheng Electric Power Economics and Technology Institute in State Grid Yancheng Power Supply Company. He is currently a registered Electrical Engineer. His research interests include power system planning and design, distributed power, and energy storage.